CHAPTER V

Thermophysical properties of the binary mixtures of 2-ethyl-1-hexanol with 1, 2-disubstituted ethanes at T = (298.15- 318.15) K

5.1. Introduction

The molecular interactions, operating between different liquids in liquid-liquid systems, control their physico-chemical properties and are of major significance in relation to their industrial applications.[1,2] The information based on density and viscosity of pure liquid and their mixtures are important for both practical and theoretical purposes. The excess properties of the binary mixtures reflect the extent of deviation in their properties from ideality and can be successfully employed in understanding the nature and the strength of the molecular interactions in such mixtures. Again ultrasonic study of the liquid systems containing the pure liquids and their mixtures has gained much importance in assessing the nature of molecular interactions and investigating the physicochemical behavior of such systems. The variation of ultrasonic speed along with the derived acoustic properties, specially their excess or deviation properties, are more useful in understanding the interactions between the molecules as they are related with structural effects and packing phenomena.[3-6] The refractive index measurements[7] are also used to estimate the different parameters like the molar refraction and the excess molar refraction which can be helpful for understanding the type of molecular interactions. Therefore the systematic investigation of the different parameters and their excess or deviation functions are of great importance for a better understanding of the liquid systems and appropriate selection of these systems for their practical applications in various industrial and biological usages. In this chapter densities and viscosities for the binary systems consisting of 2-ethyl-1-hexanol (2-EH) as component 1 and ethylenediamine (EDA), 1,2-dichloroethane (DCE) and monoethanolamine (MEA) as component 2 were measured at 298.15, 308.15 and 318.15 K. Also ultrasonic speeds of sound and refractive indices for such systems were measured at 298.15 K under atmospheric pressure. Different excess or deviation properties derived from these experimental data were discussed in terms of molecular interactions. To the best of our knowledge no volumetric, viscometric, acoustic and refractive index study is available in the

literature for the binary mixtures of 2-ethyl-1-hexanol with ethylenediamine, 1,2-dichloroethane and monoethanolamine at the experimental conditions studied.

5.2. *Experimental section*

5.2.1. *Materials*

All the chemicals chosen for this investigation were of spectroscopic grade (Sigma-Aldrich, purity>99%) and were used without any further purification as received from the vendor. The purity of each solvent was ascertained by comparing their experimental densities and viscosities at the experimental temperatures as listed in Table 5.1 with the available literature data.[8-19]

5.2.2. *Apparatus and procedure*

Different binary mixtures of the selected solvents were prepared at 298.15 K by mass and were kept in special airtight stoppered glass bottles to avoid evaporation. The mass measurements were done on a digital electronic analytical balance (Mettler, AG 285, Switzerland) with an uncertainty of $\pm 1 \cdot 10^{-4}$ g and the uncertainty in mole fraction was evaluated to be ±0.0002. The densities of the pure liquids and their binary mixtures were measured with a vibrating-tube density meter (Anton Paar, DMA 4500M). The densitometer was calibrated at the experimental temperatures using doubly distilled and degassed water and dry air under atmospheric pressure. The desired experimental temperatures were automatically kept constant with an accuracy of $\pm 1 \cdot 10^{-2}$ K by using a built–in Peltier technique. The viscosity of the pure liquids and their binary mixtures were measured using a suspended Canon-type Ubbelohde viscometer. Before use the viscometer was thoroughly cleaned, dried and calibrated at the experimental temperatures with triply distilled, degassed water and purified methanol. The efflux times of flow of liquid samples were recorded with a digital stopwatch with an uncertainty of ±0.01s. Ultrasonic speeds of sound (u) were measured at T = (298.15 ± 0.01) K with an accuracy of 0.3 % by using a variable path, single crystal ultrasonic interferometer (Mittal Enterprise, New Delhi, F-05) working at 2 MHz. Refractive indices were measured with an Abbe's refractometer at T = (298.15 ± 0.01) K. In all determinations, an average of triplicate measurements was taken into account and adequate precautions were taken to minimize evaporation loses during the actual measurements. The details of the methods, uncertainties and measurement techniques have already been described in Chapter III.

Table 5.1. Physical properties of the pure liquids at T = (298.15 to 318.15) K

Pure Liquid	T (K)	$\rho \cdot 10^{-3}$ (kg · m^{-3})		η (mPa · s)	
		Expt.	Lit.	Expt.	Lit.
2-EH	298.15	0.82907	0.82906[8] 0.82896[9]	8.4186	8.418[10]
	308.15	0.82159	0.82158[9]	6.0823	6.090[10]
	318.15	0.81413	0.81411[9]	3.7257	-
EDA	298.15	0.89479	0.8945[11] 0.8948[11]	1.2758	1.276[11]
	308.15	0.88563	0.8856[12]	1.1072	1.107[11]
	318.15	0.86762	0.867667[13]	0.9445	0.9445[14]
DCE	298.15	1.24637	1.2474[15]	0.7804	0.759[15] 0.7805[16]
	308.15	1.23121	1.2312[15]	0.6744	0.674[15]
	318.15	1.21455	1.21455[14]	0.5719	0.5719[14]
MEA	298.15	1.01179	1.0118[17]	18.9538	18.95[19]
	308.15	1.00468	1.00467[17] 1.00431[18]	11.9630	11.966[18]
	318.15	0.99815	0.99817[17] 0.99635[18]	7.9132	7.914[18]

5.3. Results and discussion

The measurement of the different physical properties of pure liquids and their binary mixtures are being used as an important tool for describing the molecular interactions operating among the unlike components of the mixture. Such studies highlight the deviation of these properties from their ideal behavior and help to investigate the molecular interactions between the unlike components in the mixture. These deviations depend upon the nature of the liquids, mixture composition and the experimental temperatures. Thus the investigation on the excess or deviation parameters helps to estimate and understand the extent of the molecular interactions operating in the mixture. The experimentally determined densities (ρ) and viscosities (η) along with the excess molar volumes (V_m^E) and viscosity deviations ($\Delta\eta$) of the binary mixtures studied at the experimental temperatures are listed in Table 5.2.

Table 5.2. Density (ρ), viscosity (η), excess molar volume (V_m^E) and viscosity deviation ($\Delta\eta$) for the binary mixtures studied at T = (298.15 to 318.15) K

x_1	$\rho \cdot 10^{-3}$ ($kg \cdot m^{-3}$)	η ($mPa \cdot s$)	$V_m^E \cdot 10^6$ ($m^3 \cdot mol^{-1}$)	$\Delta\eta$ ($mPa \cdot s$)
2-EH (1) + EDA (2)				
T = 298.15 K				
0	0.89479	1.2758	0	0
0.0488	0.88820	1.4630	-0.036	0.0641
0.1034	0.88175	1.7049	-0.080	0.1542
0.1651	0.87552	2.0516	-0.142	0.3095
0.2352	0.86941	2.4932	-0.215	0.5047
0.3157	0.86323	3.0203	-0.282	0.7057
0.4090	0.85701	3.6868	-0.345	0.9266
0.5185	0.85056	4.3758	-0.376	0.9821
0.6486	0.84376	5.1930	-0.347	0.8551
0.8059	0.83651	6.2905	-0.218	0.4536
1	0.82907	8.4186	0	0
T = 308.15 K				
0	0.88563	1.1072	0	0
0.0488	0.87910	1.2537	-0.027	0.0505
0.1034	0.87260	1.4332	-0.050	0.1127
0.1651	0.86664	1.7323	-0.119	0.2655
0.2352	0.86031	2.0719	-0.151	0.4190
0.3157	0.85419	2.5380	-0.201	0.6422
0.4090	0.84828	3.0787	-0.274	0.8563
0.5185	0.84206	3.5855	-0.307	0.9074
0.6486	0.83560	4.0757	-0.296	0.7331
0.8059	0.82864	4.7035	-0.181	0.3337
1	0.82159	6.0823	0	0
T = 318.15 K				
0	0.86762	0.9445	0	0
0.0488	0.86213	1.0491	-0.015	0.0392
0.1034	0.85673	1.1960	-0.033	0.1075
0.1651	0.85166	1.4374	-0.080	0.2527
0.2352	0.84650	1.6815	-0.117	0.3772
0.3157	0.84146	2.0221	-0.167	0.5654
0.4090	0.83639	2.4019	-0.213	0.7463
0.5185	0.83127	2.7433	-0.252	0.8192
0.6486	0.82586	2.9488	-0.243	0.6486
0.8059	0.82008	3.1463	-0.156	0.2918
1	0.81413	3.7257	0	0
2-EH (1) + DCE (2)				
T = 298.15 K				
0	1.24637	0.7804	0	0
0.0779	1.18639	0.7528	0.016	-0.1865
0.1597	1.13193	0.9344	0.034	-0.2066

0.2457	1.08261	1.2791	0.022	-0.1208
0.3363	1.03773	1.7632	-0.026	0.0266
0.4318	0.99622	2.4669	-0.051	0.2875
0.5327	0.95797	3.2867	-0.088	0.5162
0.6394	0.92248	4.2152	-0.117	0.6444
0.7525	0.88931	5.1569	-0.116	0.4839
0.8724	0.85819	6.3998	-0.067	0.1848
1	0.82907	8.4186	0	0
		T = 308.15 K		
0	1.23121	0.6744	0	0
0.0779	1.17215	0.5472	0.042	-0.2532
0.1597	1.11892	0.6466	0.052	-0.3116
0.2457	1.07068	0.8895	0.030	-0.2682
0.3363	1.02658	1.3328	-0.010	-0.0802
0.4318	0.98582	1.8869	-0.033	0.1437
0.5327	0.94825	2.6389	-0.069	0.4626
0.6394	0.91336	3.4333	-0.096	0.6813
0.7525	0.88076	4.1632	-0.097	0.6341
0.8724	0.85017	4.9219	-0.051	0.3279
1	0.82159	6.0823	0	0
		T = 318.15 K		
0	1.21455	0.5719	0	0
0.0779	1.15698	0.3641	0.046	-0.2977
0.1597	1.10499	0.4412	0.065	-0.3302
0.2457	1.05783	0.5692	0.052	-0.3371
0.3363	1.01485	0.8605	0.002	-0.2136
0.4318	0.97495	1.3005	-0.015	0.0159
0.5327	0.93818	1.8483	-0.050	0.2963
0.6394	0.90394	2.4608	-0.065	0.5653
0.7525	0.87197	2.9102	-0.061	0.5672
0.8724	0.84206	3.2181	-0.029	0.2848
1	0.81413	3.7257	0	0
		2-EH (1) + MEA (2)		
		T = 298.15 K		
0	1.01179	18.9538	0	0
0.0495	0.99182	18.3499	-0.121	0.1424
0.1049	0.97172	17.7102	-0.193	0.3046
0.1674	0.95291	17.0280	-0.312	0.4819
0.2382	0.93455	16.3047	-0.422	0.6825
0.3193	0.9165	15.5619	-0.512	0.9348
0.4020	0.90119	14.7035	-0.623	1.0259
0.5225	0.88222	13.6371	-0.711	1.2338
0.6523	0.86478	12.2476	-0.663	1.0844
0.8085	0.8469	10.4609	-0.423	0.6268
1	0.82907	8.4186	0	0
		T = 308.15 K		
0	1.00468	11.9630	0	0
0.0495	0.98394	11.6681	-0.077	0.0990

0.1049	0.96386	11.4254	-0.152	0.2826
0.1674	0.94459	11.1083	-0.235	0.4261
0.2382	0.92644	10.8491	-0.362	0.6664
0.3193	0.90856	10.5217	-0.467	0.8826
0.4020	0.89325	10.0940	-0.577	0.9793
0.5225	0.87407	9.4923	-0.635	1.0910
0.6523	0.85674	8.6493	-0.592	0.9542
0.8085	0.83907	7.4358	-0.372	0.5123
1	0.82159	6.0823	0	0
		T = 318.15 K		
0	0.99815	7.9132	0	0
0.0495	0.97677	7.6953	-0.045	0.0717
0.1049	0.95624	7.5229	-0.096	0.2115
0.1674	0.93699	7.3377	-0.185	0.3620
0.2382	0.91853	7.1545	-0.290	0.5411
0.3193	0.90064	6.9980	-0.396	0.7765
0.4020	0.88508	6.7868	-0.480	0.9411
0.5225	0.86596	6.4309	-0.542	1.0924
0.6523	0.84875	5.9254	-0.511	1.0842
0.8085	0.83135	5.0766	-0.328	0.7728
1	0.81413	3.7257	0	0

5.3.1. *Excess molar volumes*

Excess molar volume (V_m^E), a thermodynamic property, is sensitive towards the change in structure during the mixing process and can be had from the relation:

$$V_m^E = \sum_{i=1}^{2} x_i M_i (1/\rho - 1/\rho_i) \quad (1)$$

where ρ is the density of the mixture and x_i, M_i and ρ_i are the mole fraction, molar mass and density of the ith component in the mixture, respectively. The estimated uncertainty in the excess molar volumes (V_m^E) was found to be ±0.005 cm^3·mol^{-1}. The variation of excess molar volumes (V_m^E) with the mole fraction (x_1) of 2-EH at 298.15 K is depicted in Figure 5.1. It shows that the excess molar volume (V_m^E) varies in a sigmoidal fashion with the mole fraction (x_1) of 2-EH for the binary mixture (2-EH + DCE) with positive V_m^E values at $x_1 \leq$ 0.2457 and negative V_m^E values at $x_1 \geq$ 0.3363. Similar composition dependence of V_m^E values was observed at other experimental temperatures for this mixture. However, negative V_m^E values were observed for the binary mixtures (2-EH + EDA) and (2-EH + MEA) over the entire composition range

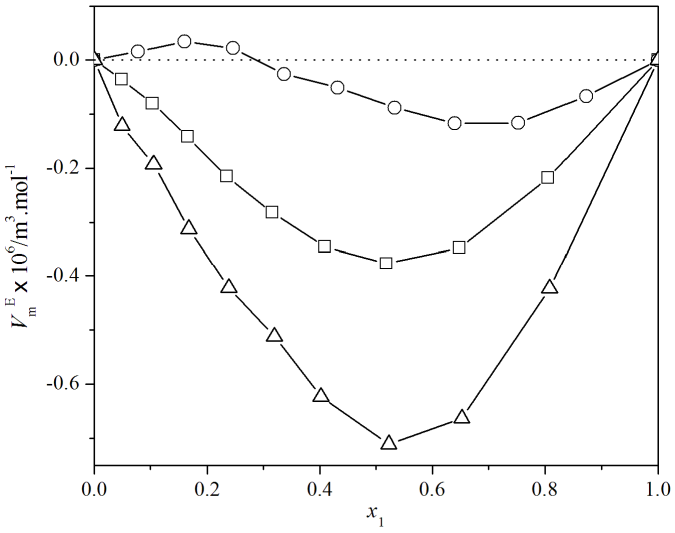

Fig. 5.1. Excess molar volume (V_m^E) *versus* mole fraction of 2-EH (x_1) for the binary mixtures of 2-EH + 1,2-disubstituted ethanes at T = 298.15 K. Symbols: □, EDA; ○, DCE; Δ, MEA.

at all the experimental temperatures. The V_m^E values can be interpreted from their sign and magnitudes reflecting the nature and the extent of the molecular interactions operating between the components of the liquid mixtures. The sign and the magnitude of V_m^E values mainly arise from the involvement of different types of interactions: physical and chemical or specific interactions. The physical interactions involve mainly the dispersion forces and cause volume expansion and thus yield positive V_m^E values. On the contrary the chemical or specific interactions that lead to volume contraction involve mainly the charge transfer type forces, hydrogen bond formation and other complex forming interactions between unlike components of the mixture and thus contribute negative values to V_m^E. Furthermore, the structural contribution that involves the geometrical fitting or interstitial accommodation of one component into other owing to their difference in molar volumes also yields negative V_m^E values. A comparison of the dipole moments (μ) and relative permittivities (ε_r)[20] of the pure components {($\mu_{2\text{-EH}}$=1.74 D, μ_{EDA}=1.99 D, μ_{DCE}=1.8 D, μ_{MEA}=2.3 D) and ($\varepsilon_{r,2\text{-EH}}$ =7.54, $\varepsilon_{r,EDA}$ =13.82, $\varepsilon_{r,DCE}$ =10.42, $\varepsilon_{r,MEA}$ =31.94)} suggests that the expected order of molecular interactions between the like components of the studied systems should be: MEA-MEA > EDA-EDA > DCE-DCE > 2-EH-2-EH. The sigmoidal variations of the V_m^E values for the mixture (2-EH + DCE) may be attributed to the breaking of the

dipolar association (through dipole-dipole interactions amongst the DCE molecules) in DCE leading to initial volume expansion ($V_m^E > 0$) on mixing with 2-EH and this effect reaches its maximum at around $x_1 = 0.2457$ and thereafter the V_m^E values drop in magnitude and become negative after $x_1 \geq 0.3363$. The negative V_m^E values for this mixture may be attributed to hydrogen bond interaction between the –OH group of 2-EH molecule and the –Cl group of DCE molecules. The other effect yielding negative V_m^E values for this system is most probably the geometrical fitting or interstitial accommodation of one component into the other due to the large differences in their sizes and molar volumes. As DCE being a smaller molecule with a molar volume of $V_{m,DCE} = 79.41$ $cm^3 \cdot mol^{-1}$ compared to 2-EH with a molar volume of $V_{m,2\text{-EH}} = 157.08$ $cm^3 \cdot mol^{-1}$ at 298.15 K, it can fit itself into the space/voids formed between the polymeric entities of 2-EH molecules[21] leading to more compact structure for the mixture (2-EH + DCE), although mixing of DCE with 2-EH also breaks intermolecular hydrogen bonds as well as dipolar associations in 2-EH.

On the contrary the negative V_m^E values for the mixtures (2-EH + EDA) and (2-EH + MEA) over the whole composition range at all the experimental temperatures suggest the presence of strong molecular interactions between the unlike components of the mixtures; most probably due to the following facts: i) the presence of highly polar $-NH_2$ and $-OH$ groups in MEA and two $-NH_2$ groups in EDA leads to hydrogen bond interactions with the $-OH$ group of 2-EH molecules on mutual mixing and ii) the geometrical fitting of EDA and MEA molecules in the intermolecular space or voids between the 2-EH molecules. This is due to difference in the size and molar volume of the participating components in the mixtures. Both EDA with a molar volume of $V_{m,EDA} = 67.15$ $cm^3 \cdot mol^{-1}$ and MEA with a molar volume of $V_{m,MEA} = 60.37$ $cm^3 \cdot mol^{-1}$ are smaller molecules than 2-EH ($V_{m,2\text{-EH}} = 157.08$ $cm^3 \cdot mol^{-1}$) and this fact permits the easy fitting of these two molecules (EDA and MEA) in the intermolecular space/voids between the 2-EH molecules and thus more compact structures result for the mixtures (2-EH + EDA) and (2-EH + MEA). Figure 5.1 reveals that V_m^E values have the following order of magnitude for the studied mixtures: (2-EH + DCE) > (2-EH + EDA) > (2-EH + MEA) irrespective of the sign of V_m^E values. This order suggests the following order of molecular

interactions: (2-EH + MEA) > (2-EH + EDA) > (2-EH + DCE). Similar behavior of the V_m^E values against the mole fraction (x_1) of 2-EH was observed for these mixtures at other experimental temperatures. However, for each mixture the V_m^E values increase as the experimental temperature increases. So it is evident that the degree of molecular interactions between the dissimilar species becomes weaker at higher temperatures; most probably due to enhanced thermal agitation and kinetic energy of the component molecules at higher temperatures.

5.3.2. ***Excess partial molar volumes***

The partial molar quantities like partial molar volume, partial molar volume at infinite dilution, *etc*., are also helpful in understanding the molecular interactions between the component molecules upon mixing. Therefore, these parameters for the ith component of the mixtures were determined at 298.15 K. The partial molar volumes ($\overline{V}_{m,i}$) of the ith component were obtained from the relation:[22,23]

$$\overline{V}_{m,i} = V_{m,i}^E + V_{m,i}^* + (1 - x_i)(dV_{m,i}^E / dx_i)_{T,P} \qquad (2)$$

where $V_{m,i}^*$ and $V_{m,i}^E$ are the molar volume and the excess partial molar volume of the ith component in the binary mixtures, respectively. The derivatives $(\partial V_{m,i}^E / \partial x_i)_{T,P}$ involved in these calculations were obtained using the excess molar volumes (V_m^E) and the Redlich-Kister coefficients (a_i)[24] of appropriate degree (as determined by Marquardt algorithm[25]). The details of these calculations are described in chapter II. The calculated Redlich-Kister coefficients (a_i) and the standard deviations (σ) are as follows a_0 = -1.4980, a_1 = -0.2488, a_2 = 0.6669 for the mixture (2-EH + EDA); a_0 = -0.3239, a_1 = -0.7469, a_2 = 0.2529, a_3 = 0.2829 for the mixture (2-EH + DCE) and a_0 = -2.7839, a_1 = -0.9154, a_2 = 0.8206, a_3 = 1.3550 for the mixture (2-EH + MEA) with standard deviations (σ) 0.0018, 0.0061, 0.0095, respectively for the mixtures (2-EH + EDA), (2-EH + DCE) and (2-EH + MEA). For a better understanding of the overall state of molecular interactions, the excess partial molar volumes ($\overline{V}_{m,i}^E$) and excess partial molar volumes ($\overline{V}_{m,i}^{0,E}$) at infinite dilution were calculated by using the standard relations described in chapter II. These parameters are more sensitive to the change in the aggregation arising due to mixing of the components. The $\overline{V}_{m,i}^E$ values of a binary

Table 5.3. Molar volumes ($V^*_{m,1}$ and $V^*_{m,2}$), partial molar volumes at infinite dilution ($\overline{V}^0_{m,1}$ and $\overline{V}^0_{m,2}$) and excess partial molar volumes at infinite dilution ($\overline{V}^{0,E}_{m,1}$ and $\overline{V}^{0,E}_{m,2}$) for each component in the binary mixtures at 298.15 K

Volume parameters	2-EH (1) +		
	EDA (2)	DCE (2)	MEA (2)
$V^*_{m,1}$	157.08	157.08	157.08
$\overline{V}^0_{m,1}$	156.49	157.47	154.68
$V^*_{m,2}$	67.15	79.41	60.37
$\overline{V}^0_{m,2}$	66.07	78.87	58.84
$\overline{V}^{0,E}_{m,1}$	-0.58	0.39	-2.40
$\overline{V}^{0,E}_{m,2}$	-1.08	-0.53	-1.52

Volume parameters are given in $cm^3 \cdot mol^{-1}$.

mixture provide valuable information regarding the individual component's response to the molecular interactions. These parameters for the studied mixtures at 298.15 K are listed in Table 5.3. The excess partial molar volumes ($\overline{V}^E_{m,i}$) for each component in the studied binaries are represented in Figure 5.2 as a function of the mole fraction (x_1) of 2-EH. Figure 5.2 shows that $\overline{V}^E_{m,1}$ values initially decrease for the mixture containing DCE (up to x_1 = 0.4318) and EDA (up to x_1 = 0.2352) and thereafter gradually increase for both the mixtures. But for the mixture with MEA $\overline{V}^E_{m,1}$ values gradually increase with increasing mole fraction (x_1) of 2-EH. However, for all the studied mixtures $\overline{V}^E_{m,2}$ values behave in opposite fashion as compared to $\overline{V}^E_{m,1}$ values as expected. Partial molar volumes ($\overline{V}^0_{m,1}$) at infinite dilution for 2-EH in the mixture (2-EH + DCE) was found to be greater than its molar volume ($V^*_{m,1}$), *i.e.*, 2-EH expands in volume but that of DCE ($\overline{V}^0_{m,2}$) was found to lower than its molar volume ($V^*_{m,2}$), *i.e.*, DCE contracts in volume. Partial molar volumes ($\overline{V}^0_{m,1}$ and $\overline{V}^0_{m,2}$) at infinite dilution for both the components in the mixtures (2-EH + EDA) and (2-EH + MEA) were also found to be lower than their respective molar volumes ($V^*_{m,1}$ and $V^*_{m,2}$). Again more negative $\overline{V}^E_{m,i}$ values for the mixture (2-EH + MEA) compared to the mixtures (2-EH + EDA) and (2-EH + DCE) are significantly more apparent and this

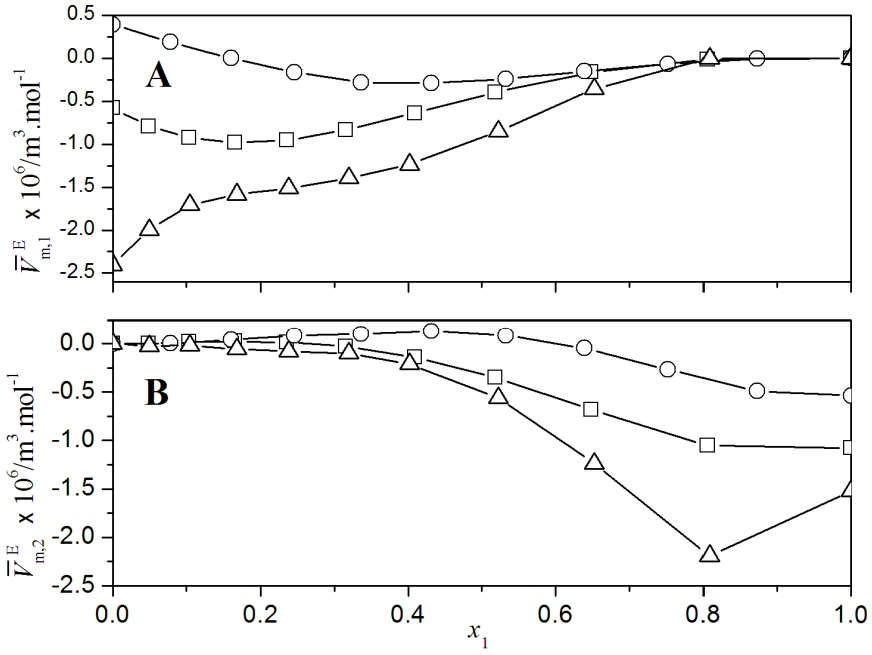

Fig. 5.2. Excess partial molar volume ($\overline{V}^{E}_{m,i}$) against mole fraction of 2-EH (x_1) for the binary mixtures of 2-EH + 1,2-disubstituted ethanes at T = 298.15 K: A, for 2-EH; B, for 1,2-disubstituted ethanes. Symbols: □, EDA; ○, DCE; Δ, MEA.

fact supports comparatively more compact structure for the mixture (2-EH + MEA) than other two mixtures. These results suggest the interstitial accommodation of these disubstituted ethanes in the voids of 2-EH ensemble and thus corroborates with the following order of packing efficiency or structure compactness in the mixtures:
(2-EH + MEA) > (2-EH + EDA) > (2-EH + DCE).

5.3.3. *Predictions of excess molar volumes*

Of late several theoretical models have been used to correlate the experimental and theoretical excess molar volumes (V^{E}_{m}). Herein this chapter Prigogine-Flory-Patterson (PFP) theory[26,27] and the Peng Robinson equation of state[28-31] at 298.15 K were used for the studied binary mixtures.

i) *Prigogine-Flory-Patterson theory* (PFP):

The Prigogine-Flory-Patterson (PFP) theory[26,27] is a modified version of Flory's statistical theory and has been successfully tested to correlate and analyze the excess thermodynamic functions like excess molar volume (V^{E}_{m}) of the liquid mixtures theoretically. According to this theory the excess molar volume (V^{E}_{m})

originates from a combination of interactional, a free volume and internal pressure combinations and V_m^E is given by:

$$\frac{V_m^E}{x_1V_1^* + x_2V_2^*} = \frac{(\tilde{v}^{1/3}-1)\tilde{v}^{2/3}\psi_1\theta_2}{[(4/3)\tilde{v}^{-1/3}-1]P_1^*}\chi_{1,2} \quad (\chi_{1,2}\text{ contribution})$$
$$- \frac{(\tilde{v}_1-\tilde{v}_2)^2[(14/9)\tilde{v}^{-1/3}-1]\psi_1\psi_2}{[(4/3)\tilde{v}^{-1/3}-1]\tilde{v}} \quad (\tilde{v}\text{ contribution})$$
$$+ \frac{(\tilde{v}_1-\tilde{v}_2)(P_1^*-P_2^*)\psi_1\psi_2}{(P_1^*\psi_2+P_2^*\psi_1)} \quad (P^*\text{ contribution}) \qquad (3)$$

The first term on the right hand side of the Eq. (3) relates to the interactional contribution, the second term relates to free volume contribution and the last term is the internal pressure contribution. The different parameters (θ, ψ and P^*) involved in Eq. (3) are the molecular surface fraction, molecular contact energy fraction and characteristic pressure respectively. The other terms and notations involved in this theory for the pure components and their mixtures were obtained using Flory's theory[28-31] and are given in Table 5.4.

Table 5.4. Isobaric molar heat capacities (c_P), expansion coefficient (α), isothermal compressibility (κ_T) and Flory's parameters for pure liquids at 298.15 K

Liquids	c_P [a]	$\tilde{v}$	$\tilde{T}$	$V^* \cdot 10^6$ ($m^3 \cdot mol^{-1}$)	P^*(Pa)	T^*(K)	$\alpha \cdot 10^4$ (K^{-1})	$\kappa_T \cdot 10^{10}$ (Pa^{-1})
2-EH	317.50[9]	1.2271	0.0537	128.01	496.96	5548.96	9.010	8.139
EDA	172.60[20]	1.3451	0.0699	49.93	1226.52	4262.04	15.182	6.677
DCE	128.40[20]	1.3018	0.0646	60.99	746.81	4611.90	12.765	8.636
MEA	195.50[20]	1.1768	0.0449	51.30	737.98	6641.29	6.740	3.771

[a] Unit : $J \cdot K^{-1} \cdot mol^{-1}$.

For the prediction of V_m^E values the interaction parameter ($\chi_{1,2}$) is required and so it was obtained by fitting the experimental equimolar ($x_1 \approx 0.5$) V_m^E values to Eq. (3) by using computer program as detailed in chapter II. The theoretically calculated and experimentally obtained excess molar volumes, their deviation and the optimized $\chi_{1,2}$ value near equimolar ($x_1 \approx 0.5$) composition for the studied binaries at 298.15 K are given in Table 5.5. It suggests that the calculated excess molar volumes ($V_{m,PFP}^E$)

Table 5.5. Interaction parameter ($\chi_{1,2}$), calculated and experimental values of excess molar volumes ($V^{E}_{m,exp}$ and $V^{E}_{m,PFP}$), their deviations (ΔV^{E}_{m}) and different PFP contributions at 298.15 K

2-EH (1) +	$\chi_{1,2}$	$V^{E}_{m,exp}\cdot 10^{6}$	$V^{E}_{m,PFP}\cdot 10^{6}$	$\Delta V^{E}_{m}\cdot 10^{6}$	PFP contributions x 10^{3}		
	($J\cdot m^{-3}$)	($m^{3}\cdot mol^{-1}$)	($m^{3}\cdot mol^{-1}$)	($m^{3}\cdot mol^{-1}$)	int[a]	fv[b]	ip[c]
DA (2)	-149.559	-0.3763	-0.3182	-0.0581	-0.0233	0.0052	0.0243
DCE (2)	-32.092	-0.0880	-0.0497	-0.0383	-0.0057	0.0020	0.0068
MEA (2)	-11.657	-0.7110	-0.6211	-0.0899	-0.0027	0.0009	-0.0042

[a] interaction contribution, [b] free volume contribution and [c] internal pressure contribution

do not agree well with the experimental excess molar volumes (V^{E}_{m}) for all the mixtures studied.

ii) *Peng-Robinson Equation of State* (PREOS):

In recent years the cubic equation of states has gained more importance because of their simplicity, computational efficiency, reliability and their easy application in the liquid mixtures through mixing or combination rules. These equations of state are commonly used to describe the phase equilibria of hydrocarbon system and finds wide applications in the prediction of properties of the solution. In the present chapter the classical cubic Peng-Robinson equation of state (PREOS) has been used to predict the excess molar volume ($V^{E}_{m,\,PREOS}$) of the mixtures at 298.15 K. The general form of the two parameter PREOS is given by:[32]

$$P=\frac{RT}{V-b}-\frac{a}{V(V+b)+b(V-b)} \tag{4}$$

where *a* and *b* are the attraction parameter and van der Waals co-volume parameters, respectively. *a* and *b* can be obtained by using the standard relations as described in chapter II. For the pure components:

$$a=a(T)=a(T_c)\left[1+\xi\left(1-\sqrt{\frac{T}{T_c}}\right)\right]^{2} \tag{5}$$

$$b=b(T)=b(T_c) \tag{6}$$

$$a(T_c)=0.45724\frac{R^{2}T_c^{2}}{P_c} \tag{7}$$

$$b(T_c)=0.07780\frac{RT_c}{P_c} \tag{8}$$

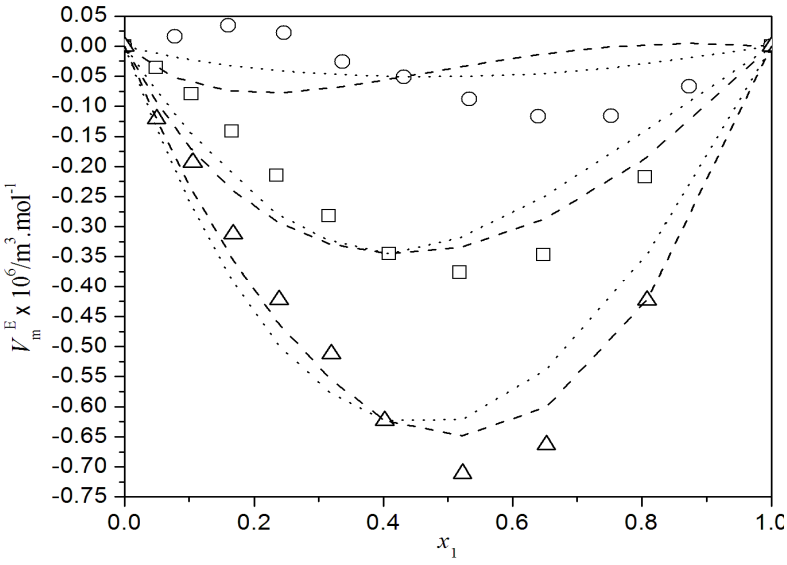

Fig. 5.3. A comparison between the excess molar volumes (V_m^E) against mole fraction of 2-EH (x_1) for the binary mixtures of 2-EH + 1,2-disubstituted ethanes at T = 298.15 K. Symbols represent experimental excess molar volumes (V_m^E): □, EDA; ○, DCE; Δ, MEA. Dashed lines and dotted lines represent excess molar volumes (V_m^E) obtained form PREOS and PFP theory, respectively.

where T_c and P_c are critical temperature and pressure of the pure components. The parameter ξ can be defined in terms of acentric factor (ω)[33] as:

$$\xi = 0.37464 + 1.54226\omega - 0.26992\omega^2 \quad (9)$$

The parameters (T_c, P_c and ω) for the pure components were taken from the literature.[20,33] For the binary mixtures the attraction parameter a and co-volume parameter b were calculated using the following standard relation:[33]

$$a(T) = \sum_{i=1}^{2}\sum_{j=1}^{2} x_i x_j \sqrt{a_i a_j}(1 - k_{ij}) \quad (10)$$

$$b(T) = \sum_{i=1}^{2} x_i b_i \quad (11)$$

where k_{ij} is the interaction coefficient of the components i and j for a binary mixture. Rearrangement of Eq. (4) in terms of compressibility factor yields:

$$Z^3 - (1-B)Z^2 + (A - 3B^2 - 2B)Z - (AB - B^2 - B^3) = 0 \quad (12)$$

In Eq. (12) the terms, $Z = PV/RT$, $A = aP/(RT)^2$ and $B = Pb/RT$. Thus from the knowledge of the compressibility factor (Z) for pure components and their mixtures, the corresponding volumes and the excess molar volumes of the systems were calculated. The interaction coefficient (k_{ij}) for the mixtures (2-EH + EDA), (2-EH + DCE) and (2-EH + MEA) were found to be -0.1668, -0.0624 and -0.1235 with standard deviations (σ) 0.0661, 0.0866 and 0.0441, respectively. The experimental excess molar volumes (V_m^E) and the calculated excess molar volumes ($V_{m,PFP}^E$ and $V_{m,PREOS}^E$) as a function of mole fraction (x_1) of 2-EH in the present system at 298.15 K are depicted in Figure 5.3. It reveals that the calculated excess molar volumes ($V_{m,PFP}^E$ and $V_{m,PREOS}^E$) although agree to some extent with the experimental excess molar volumes (V_m^E) for the mixtures (2-EH + EDA) and (2-EH + MEA) but for the mixture (2-EH + DCE), both the models (PREOS and PFP) fail to predict its excess molar volumes.

5.3.4. *Viscosity deviations*

The study of transport properties of the liquid mixture is very useful in process design, development of the liquid state theories and predictive methods, *etc*. Viscosity deviation ($\Delta\eta$) depends on the strength of intermolecular hydrogen bonding, molecular size and shape of the components. Hence it is very important and useful tool for understanding the nature of intermolecular interactions between the unlike components. Therefore, the viscosity deviations ($\Delta\eta$) of all the studied binaries were evaluated at T = (298.15-318.15) K from the relation:[34]

$$\Delta\eta = \eta - \eta_{id} \tag{13}$$

where η_{id} is the ideal viscosity of the solution as given by:[35]

$$\eta_{id} = \exp\left(\sum_{i=1}^{2} x_i \ln \eta_{id}\right) \tag{14}$$

Figure 5.4 ($\Delta\eta$ *versus* x_1 at 298.15 K) shows that the $\Delta\eta$ values are positive for the mixtures (2-EH + EDA) and (2-EH+MEA) over the entire composition range. However, for the mixture (2-EH + DCE), $\Delta\eta$ values vary in a sigmoidal fashion with negative $\Delta\eta$ values at the lower mole fraction of 2-EH (up to $x_1 \leq 0.2457$) and positive $\Delta\eta$ values at 2-EH rich regions ($x_1 \geq 0.2457$). Similar composition dependence of $\Delta\eta$ values was observed at other experimental temperatures for these mixtures.

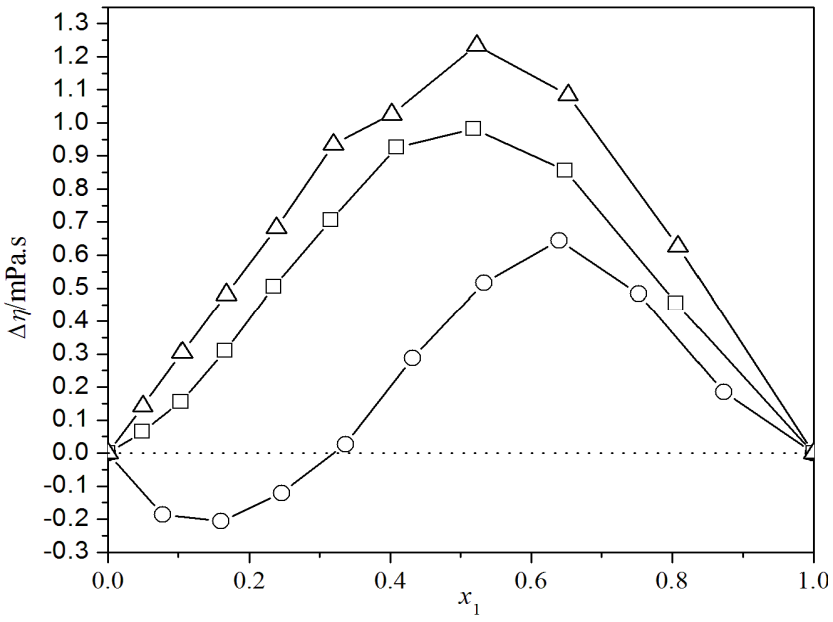

Fig. 5.4. Viscosity deviation ($\Delta\eta$) *versus* mole fraction of 2-EH (x_1) for the binary mixtures of 2-EH + 1,2-disubstituted ethanes at T = 298.15 K. Symbols represent experimental points: □, EDA; ○, DCE; Δ, MEA.

For many liquid-liquid systems the $\Delta\eta$ *versus* x_1 plot often shows a reversed trend compared to the V_m^E *versus* x_1 plots; *i.e.*, if V_m^E is positive $\Delta\eta$ will be negative and *vice -versa*.[36] Such a coincidence was observed for all the studied binaries. According to Vogel and Weiss,[37] viscosity deviations are positive for mixtures with strong molecular interactions and negative for the mixtures without specific interaction or with weak interactions. The negative $\Delta\eta$ values for the mixture (2-EH + DCE) at dilute 2-EH regions is most probably due to loss of dipolar association of DCE on mixing with 2-EH. But at 2-EH rich regions $\Delta\eta$ values gradually increase and become positive suggesting predominance of specific interactions like dipole-dipole interactions, hydrogen bond interaction and interstitial accommodation or geometrical fitting as described earlier. The positive $\Delta\eta$ values for the mixtures (2-EH + EDA) and (2-EH + MEA) over the entire composition range entails that these two binary mixtures are characterized by strong molecular interactions (amongst the dissimilar species) arising out of specific dipole-dipole interactions, hydrogen bonds and interstitial accommodation. Thus the $\Delta\eta$ values also suggest the same order of molecular interactions for the mixtures as discussed earlier. Anyway, for each mixture

$\Delta\eta$ values decrease at higher temperatures reflecting the fact that the molecular interactions amongst the dissimilar species become weaker at higher temperatures.

5.3.5. ***Thermodynamics of viscous flow***

According to Eyring's viscosity relation,[35] the free energy of viscous flow (ΔG^*) is given by the relation:

$$\eta = (hN/V)\exp(\Delta G^*/RT) \tag{15}$$

where h is Planck's constant, N is Avogadro's number and other symbols have their usual meanings. Rearranging Eq. (15) and putting $\Delta G^* = \Delta H^* - T\Delta S^*$ yields the following relation:

$$R\ln(\eta V/hN) = \Delta H^*/T - \Delta S^* \tag{16}$$

Thus, linear regressions of $R\ln(\eta V/hN)$ against $(1/T)$ give the enthalpy (ΔH^*) and entropy (ΔS^*) of activation of viscous flow from the corresponding slope and negative intercept, respectively. ΔG^*, ΔH^*, ΔS^* and the regression coefficients (R^2) are given in Table 5.6. It shows that while ΔH^* and ΔS^* values are positive for the mixtures (2-EH + DCE) and (2-EH + MEA), the ΔS^* values are mostly negative for the binary mixtures (2-EH + EDA) except at $x_1 \geq 0.6486$. Such a trend in ΔH^* and ΔS^* values indicate that formation of transition state for viscous flow is accompanied by disruption of the dipolar association as well as specific interactions between the components of the mixtures. According to Corradini *et al.*,[38] the enthalpy of activation of viscous flow is regarded as a measure of the degree of cooperation between the species involved in viscous flow. In a highly structured liquid there will be considerable degree of order; hence for cooperative movement of the species a large heat of activation is required for the viscous flow. Thus the ΔH^* values indicate that the molecular compactness follows the order: (2-EH + MEA) > (2-EH + + EDA) > (2-EH + + DCE). This order is also supported by the ΔS^* values for the mixtures studied. The ΔG^{*E} values are plotted against the mole fraction of 2-EH (x_1) in Figure 5.5 at 298.15 K. Reid and Taylor[39] suggested that the positive ΔG^{*E} stands for molecular interactions or compactness due to geometrical fittings of one component into the other on mixing and negative ΔG^{*E} indicate the dominance of dispersion forces in the mixtures. From Figure 5.5 it is evident that the ΔG^{*E} values for the mixtures stand in support of the order of the molecular interactions discussed above.

Table 5.6. Free energy (ΔG^*), enthalpy (ΔH^*) and entropy (ΔS^*) of activation of viscous flow for the binary mixtures.

x_1	ΔG^* ($kJ \cdot mol^{-1}$)			ΔH^* ($kJ \cdot mol^{-1}$)	ΔS^* ($J \cdot K^{-1} \cdot mol^{-1}$)	R^2
	298.15 K	308.15 K	318.15 K			
2-EH (1) + EDA (2)						
0	13.309	13.419	13.488	10.634	-8.995	0.9988
0.0488	13.804	13.898	13.929	11.928	-6.325	0.9978
0.1034	14.347	14.410	14.448	12.840	-5.066	0.9999
0.1651	14.978	15.073	15.114	12.931	-6.893	0.9987
0.2352	15.643	15.720	15.721	14.466	-3.988	0.9978
0.3157	16.312	16.440	16.413	14.788	-5.195	0.9913
0.4090	17.014	17.149	17.086	15.903	-3.829	0.9879
0.5185	17.663	17.771	17.674	17.473	-0.745	0.9892
0.6486	18.332	18.351	18.121	21.428	10.256	0.9895
0.8059	19.075	18.994	18.574	26.480	24.662	0.9872
1	20.093	19.957	19.332	31.346	37.488	0.9812
2-EH (1) + DCE (2)						
0	12.506	12.583	12.591	11.226	-4.330	0.9971
0.0779	12.599	12.236	11.590	27.605	50.182	0.9918
0.1597	13.313	12.846	12.285	28.624	51.305	0.9991
0.2457	14.265	13.842	13.142	30.968	55.877	0.9938
0.3363	15.231	15.053	14.414	27.332	40.345	0.9781
0.4318	16.231	16.116	15.684	24.341	27.034	0.9868
0.5327	17.108	17.146	16.788	21.809	15.560	0.9748
0.6394	17.889	17.989	17.719	20.361	8.096	0.9747
0.7525	18.552	18.651	18.335	21.714	10.389	0.9721
0.8724	19.250	19.247	18.774	26.282	23.337	0.9753
1	20.093	19.957	19.332	32.346	37.488	0.9812
2-EH (1) + MEA (2)						
0	19.734	19.235	18.783	33.915	47.589	0.9998
0.0495	19.838	19.364	18.911	33.667	46.394	0.9999
0.1049	19.944	19.511	19.060	33.125	44.199	0.9999
0.1674	20.047	19.648	19.210	32.524	41.828	0.9999
0.2382	20.150	19.804	19.368	31.784	38.974	0.9994
0.3193	20.255	19.954	19.546	30.808	35.337	0.9991
0.4020	20.321	20.062	19.687	29.755	31.579	0.9988
0.5225	20.410	20.190	19.840	28.885	28.358	0.9984
0.6523	20.412	20.229	19.910	27.870	24.945	0.9981
0.8085	20.313	20.143	19.812	27.752	24.866	0.9973
1	20.093	19.957	19.332	31.346	37.488	0.9812

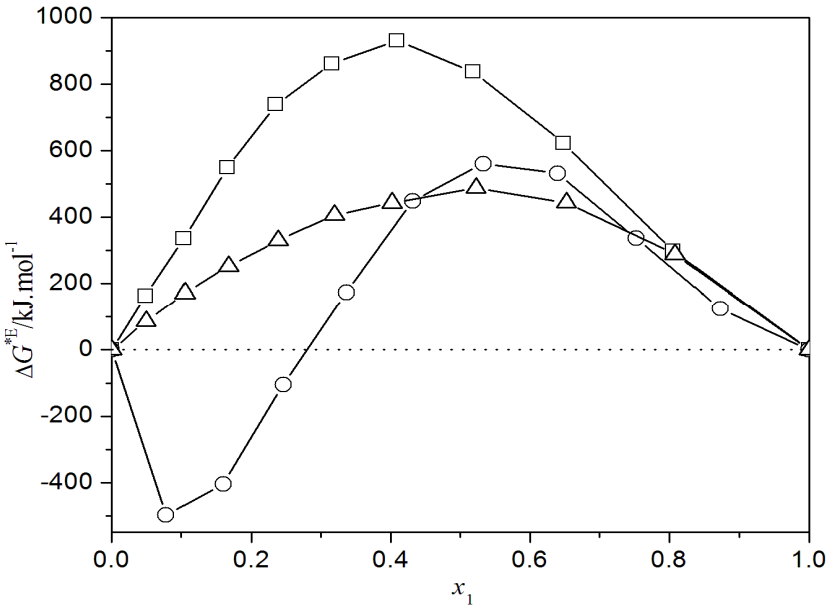

Fig. 5.5. Excess free energy of activation of viscous flow (ΔG^{*E}) *versus* mole fraction of 2-EH (x_1) for the binary mixtures of 2-EH + 1,2-disubstituted ethanes at T = 298.15 K. Symbols represent experimental points: □, EDA; ○, DCE; Δ, MEA.

5.3.6. *Viscosity prediction*

Several theoretical models, empirical and semi empirical based relations have been proposed to represent the dependence of viscosity on mole fraction in binary liquid mixtures. The simulation of the viscosity of liquid mixtures can be obtained by the use of these empirical models. Mehrotra *et al*[40] have reviewed the practical implication of these models. Such empirical models have also been developed based on van der waals' theory and the corresponding state principle by using the reduced thermodynamic properties of the substances.[41] In the present chapter the viscosities of the binary liquid mixtures were theoretically evaluated and correlated with the experimental viscosities using the cubic equation of state based on Peng-Robinson model[32] and the Bloomfield-Dewan model[42] at 298.15 K.

i) *Viscosity model using Peng-Robinson Equation of State*:

According to this model, the viscosity of a mixture is given by:

$$\eta = \frac{(\eta V)^{id}}{V_m} \exp\left[\sum_{i=1}^{2} x_i (\ln \varphi_i - \ln \varphi_i^0) + \frac{1}{2}\sum_{i=1}^{2}\sum_{j=1}^{2} x_i x_j g_{ij}\right] \quad (17)$$

This expression is a combination of Eyring's viscosity expression with the Peng-Robinson equation of state. In Eq. (17) V_m, $(\eta V)^{id}$, φ_i^0, φ_i and g_{12} are the molar volume, kinematic viscosity of an ideal mixture, fugacity coefficient of the ith component in pure state, fugacity coefficient of the ith component in a binary mixture and the binary interaction parameter, respectively. $(\eta V)^{id}$ can be had from the expression:

$$(\eta V)^{id} = \exp\left[\sum_{i=1}^{2} x_i \ln(\eta_i V_i)\right] \tag{18}$$

According to PREOS, fugacity coefficient for a pure component and for the ith component in their binary mixture are given by:

$$\ln\varphi^0 = (Z-1) - \ln(Z-B) - \frac{A}{2\sqrt{2}B}\ln\left(\frac{Z+(1+\sqrt{2})B}{Z+(1-\sqrt{2})B}\right) \tag{19}$$

$$\ln\varphi_i = \frac{b_i}{b}(Z-1) - \ln(Z-B) - \frac{A}{2\sqrt{2}B}\left(\frac{2}{a}\sum_{j=1}^{2} x_j (a_i a_j)^{\frac{1}{2}}(1-k_{ij}) - \frac{b_i}{b}\right)\ln\left(\frac{Z+(1+\sqrt{2})B}{Z+(1-\sqrt{2})B}\right) \tag{20}$$

The inter relationship between the binary interaction parameter g_{12} ($g_{ii} = 0$ and $g_{ij} = g_{ji}$) and the excess activation free energy of viscous flow, ΔG^{*E} is given by:

$$\frac{\Delta G^{*E}}{RT} = \frac{G^{*E}}{RT} + \frac{1}{2}\sum_{i=1}^{2}\sum_{j=1}^{2} x_i x_j g_{ij} = \frac{G^{*E}}{RT} + x_1 x_2 g_{12} \tag{21}$$

and ΔG^{*E} were obtained from the relation:[34]

$$\Delta G^{*E} = \Delta G^{*} - \sum_{i=1}^{2}(x_i \Delta G_i^{*}) \tag{22}$$

The binary interaction parameters (g_{12}) were obtained from a C-program utilizing a non-linear regression analysis to yield minimum standard deviations (σ) between the experimental and the calculated viscosities for the studied mixtures. The binary interaction parameters (g_{12}) were found to be 0.423 (σ = 0.029), 0.338 (σ = 0.145) and 0.027 (σ =0.014) for the mixtures (2-EH + EDA), (2-EH + DCE) and (2-EH + MEA), respectively.

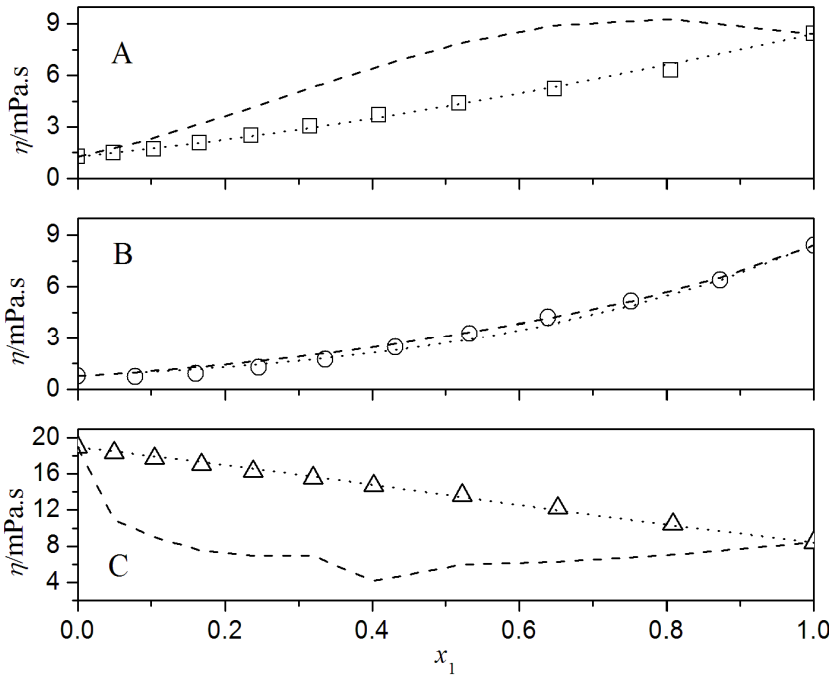

Fig. 5.6. A comparison between the viscosities (η) against mole fraction of 2-EH (x_1) for the binary mixtures of 2-EH + 1,2-disubstituted ethanes at T = 298.15 K. Symbols represent experimental viscosities: □, EDA; ○, DCE; Δ, MEA. Dashed lines and dotted lines represent viscosities (η) obtained form Bloom Field-Dewan theory and PREOS, respectively.

ii) *Bloomfield-Dewan viscosity model:*

Bloomfield and Dewan proposed a viscosity model based on the free-volume theory[42] and the absolute reaction rate theory.[35] All the involved thermodynamic parameters used in this model were evaluated using Flory's statistical thermodynamic theory for liquid mixtures.[28-31] The statistical theory from which this equation of state evolved treats the properties of a mixture in terms of reduced properties of the pure components. The proposed expression for the viscosity is given by:

$$\Delta \ln \eta = f(\tilde{v}) - \frac{\Delta G^{R}}{RT} \qquad (23)$$

where $f(\tilde{v})$ and ΔG^{R} are the characteristic function of the free volume and the residual free energy of mixing, respectively and $\Delta \ln \eta$ is given by the expression:

$$\Delta \ln \eta = \ln \eta - \sum_{i=1}^{2} (x_i \eta_i) \qquad (24)$$

$f(\tilde{v})$ and ΔG^{R} were evaluated using the following standard relations:[42]

$$f(\tilde{v}) = \frac{1}{\tilde{v} - 1} - \sum_{i=1}^{2} \frac{x_i}{\tilde{v}_i - 1} \tag{25}$$

$$\Delta G^R = \Delta G^E + RT \sum_{i=1}^{2} x_i \ln(x_i / \phi_i) \tag{26}$$

where ϕ_i is the segment fraction of the ith component in a binary mixture.[28-31] The excess energy ΔG^E in the above expression can be obtained from the Flory's statistical theory using the relation:

$$\Delta G^E = \sum_{i=1}^{2} x_i P_i^* V_i^* [(1/\tilde{v}_i - 1/\tilde{v}) + 3\tilde{T}_i \ln\{(\tilde{v}_i^{1/3} - 1)/(\tilde{v}^{1/3} - 1)\}] + (x_1 \theta_2 V_1^* \chi_{12})/\tilde{v} \tag{27}$$

The estimating ability of this model was tested by calculating the standard deviations (σ) between the experimental and the calculated viscosities and the standard deviations (σ) were found to be 2.56, 0.25 and 8.66 for the mixtures with EDA, DCE and MEA, respectively. A comparison of the experimental viscosities with the viscosities calculated from these two viscosity prediction models has been illustrated in Figure 5.6. It reveals that the model based on PREOS better predicted the viscosities for all the studied mixtures than the Bloomfield-Dewan model.

5.3.7. ***Ultrasonic speed of sound and derived functions*****:**

The ultrasonic studies can provide valuable information regarding the strength of molecular interactions in pure liquids and their mixtures. Therefore the measurement of ultrasonic speeds has become one of the important tools to estimate the nature and the strength of the molecular interactions in the binary liquid mixtures. Concentration dependence of the isentropic compressibility (κ_S) and other acoustic properties can impart valuable information about molecular interactions and structural aspects in the binary mixtures. Hence using the experimentally measured densities (ρ) and speed of sound (u) of the binary mixtures at 298.15 K the isentropic compressibility (κ_S), intermolecular free length (L_f), acoustic impedance (z_{im}) and their excess or deviation functions were determined. The variation of these excess or deviation functions with the mole fraction (x_1) of 2-EH provides better understanding of the molecular interactions between the components of the binary mixtures. The excess isentropic compressibility (κ_S^E) can be determined from the relation:

$$\kappa_S^E = \kappa_S - \kappa_S^{id} \tag{28}$$

The isentropic compressibility, κ_S in the above expression was calculated using the Laplace relation:[43]

$$\kappa_S = 1/\rho u^2 \tag{29}$$

The experimental speeds of sound for the pure liquids were in good agreement with the literature values[8,17,44,45] at 298.15 K. According to Benson and Kiyohara[46] and Acree,[47] the isentropic compressibility (κ_S^{id}) for an ideal mixture is given by:

$$\kappa_S^{id} = \sum_{i=1}^{2} \tau_i \left[\kappa_{S,i} + \frac{T V_{m,i}^{*} \alpha_i^2}{c_{P,i}} \right] - \left\{ \frac{T \sum_{i=1}^{2} (x_i V_{m,i}^{*}) \sum_{i=1}^{2} (\tau_i \alpha_i)^2}{\sum_{i=1}^{2} (x_i c_{P,i})} \right\} \tag{30}$$

where, τ_i is the volume fraction of the i[th] component in the mixture, $\kappa_{S,i}$, $V_{m,i}^{*}$, α_i and $c_{P,i}$ are the isentropic compressibility, the molar volume, the expansion coefficient and the molar isobaric heat capacity of the pure components, respectively. The experimental densities were used to calculate the expansion coefficients ($\alpha = -\rho^{-1}(d\rho/dT)_P$) and the $c_{P,i}$ values (required for the calculation) were taken from the literature.[9,20] The speed of sound (u), isentropic compressibility (κ_S) and excess isentropic compressibility parameters (κ_S^E), at 298.15 K are given in Table 5.7. Figure 5.7 illustrates the excess isentropic compressibilities (κ_S^E) of the studied mixtures against the mole fraction (x_1) of 2-EH at 298.15 K. While κ_S^E values for the mixtures (2-EH + EDA) and (2-EH + MEA) were found to be negative over the entire composition range, those for the mixture (2-EH + DCE) followed a sigmoid trend with positive κ_S^E values at DCE rich regions but with negative κ_S^E values at 2-EH rich regions. The descending order of negative κ_S^E values for the studied mixtures indicates enhanced rigidity or more efficient packing of the dissimilar species in the mixtures.[36] The intermolecular free length (L_f), specific acoustic impedance (z_{im}) and their excess functions were determined using the standard relations (detailed in Chapter II). Intermolecular free length (L_f), acoustic impedance (z_{im}) and their excess functions at 298.15 K are given in Table 5.8. The L_f^E and z_{im}^E values are depicted in Figure 5.8 against the mole fraction (x_1) of 2-EH at 298.15 K.

Table 5.7. Ultrasonic speeds (u), isentropic compressibility (κ_S) and excess isentropic compressibility (κ_S^E) for binary mixtures at 298.15 K

x_1	u ($m \cdot s^{-1}$)	$\kappa_S \times 10^{10}$ (Pa^{-1})	$\kappa_S^E \times 10^{10}$ (Pa^{-1})
2-EH (1) + EDA (2)			
0	1670.8	4.003	0
0.0488	1666.2	4.055	-0.275
0.1034	1653.4	4.149	-0.501
0.1651	1636.1	4.267	-0.695
0.2352	1619.5	4.385	-0.881
0.3157	1598.8	4.532	-1.032
0.4090	1569.8	4.735	-1.119
0.5185	1530.4	5.020	-1.117
0.6486	1475.1	5.447	-0.965
0.8059	1395.7	6.137	-0.544
1	1318.2	6.941	0
2-EH (1) + DCE (2)			
0	1193.6	5.632	0
0.0779	1179.8	6.056	0.152
0.1597	1195.4	6.182	0.061
0.2457	1228.0	6.125	-0.174
0.3363	1272.5	5.951	-0.494
0.4318	1310.0	5.849	-0.717
0.5327	1334.8	5.859	-0.809
0.6394	1346.0	5.983	-0.770
0.7525	1342.3	6.241	-0.585
0.8724	1325.9	6.628	-0.260
1	1318.2	6.941	0
2-EH (1) + MEA (2)			
0	1716.8	3.353	0
0.0495	1735.0	3.349	-0.470
0.1049	1740.1	3.399	-0.860
0.1674	1735.2	3.485	-1.188
0.2382	1720.0	3.617	-1.447
0.3193	1697.1	3.788	-1.643
0.4020	1660.3	4.025	-1.714
0.5225	1611.7	4.364	-1.736
0.6523	1538.1	4.888	-1.513
0.8085	1435.6	5.729	-0.952
1	1318.2	6.941	0

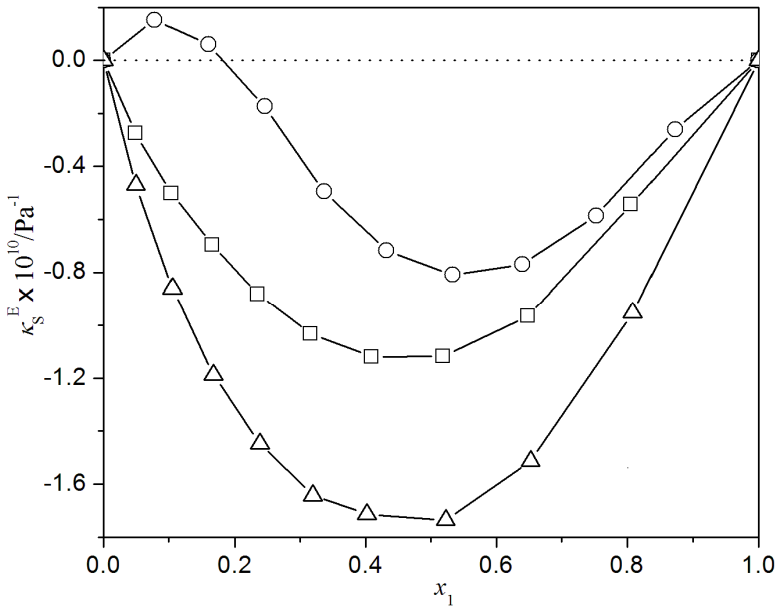

Fig. 5.7. Excess isentropic compressibility (κ_S^E) *versus* mole fraction of 2-EH (x_1) for the binary mixtures of 2-EH + 1,2-disubstituted ethanes at T = 298.15 K. Symbols: □, EDA; ○, DCE; Δ, MEA.

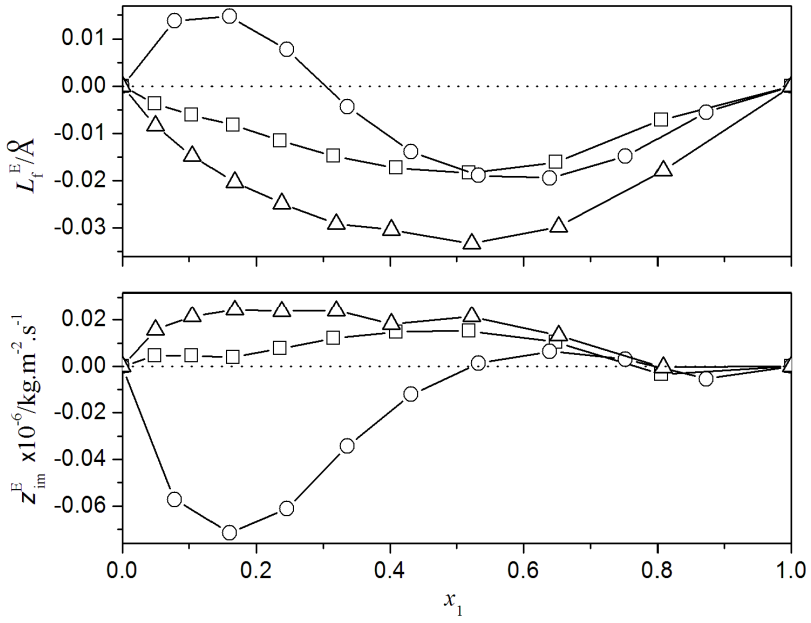

Fig. 5.8. Excess intermolecular free length (L_f^E) and excess acoustic impedances (z_{im}^E) *versus* mole fraction of 2-EH (x_1) for the binary mixtures of 2-EH + 1,2-disubstituted ethanes at T = 298.15 K. Symbols: □, EDA; ○, DCE; Δ, MEA.

Table 5.8. Intermolecular free length (L_f), specific acoustic impedance (z_{im}), excess intermolecular free lengths (L_f^E) and excess acoustic impedances (z_{im}^E) for the studied binaries at 298.15 K

x_1	L_f (Å)	$z_{im} \cdot 10^{-6}$ ($kg \cdot m^{-2} \cdot S^{-1}$)	L_f^E (Å)	$z_{im}^E \cdot 10^{-6}$ ($kg \cdot m^{-2} \cdot S^{-1}$)
2-EH (1) + EDA (2)				
0	0.4115	1.4950	0	0
0.0488	0.4142	1.4799	-0.0037	0.0045
0.1034	0.4189	1.4579	-0.0061	0.0045
0.1651	0.4249	1.4324	-0.0082	0.0038
0.2352	0.4307	1.4080	-0.0115	0.0076
0.3157	0.4379	1.3801	-0.0148	0.0121
0.4090	0.4476	1.3453	-0.0173	0.0148
0.5185	0.4608	1.3017	-0.0183	0.0152
0.6486	0.4800	1.2446	-0.0161	0.0104
0.8059	0.5095	1.1675	-0.0071	-0.0034
1	0.5419	1.0929	0	0
2-EH (1) + DCE (2)				
0	0.4881	1.4877	0	0
0.0779	0.5061	1.3997	0.0138	-0.0572
0.1597	0.5114	1.3531	0.0147	-0.0715
0.2457	0.5090	1.3294	0.0077	-0.0612
0.3363	0.5018	1.3205	-0.0044	-0.0344
0.4318	0.4974	1.3050	-0.0139	-0.0121
0.5327	0.4979	1.2787	-0.0189	0.0013
0.6394	0.5031	1.2417	-0.0194	0.0064
0.7525	0.5138	1.1937	-0.0148	0.0031
0.8724	0.5295	1.1379	-0.0055	-0.0054
1	0.5419	1.0929	0	0
2-EH (1) + MEA (2)				
0	0.3766	1.7370	0	0
0.0495	0.3764	1.7208	-0.0084	0.0157
0.1049	0.3792	1.6909	-0.0148	0.0215
0.1674	0.3840	1.6535	-0.0203	0.0243
0.2382	0.3912	1.6074	-0.0248	0.0238
0.3193	0.4003	1.5554	-0.0291	0.0240
0.4020	0.4127	1.4962	-0.0304	0.0182
0.5225	0.4297	1.4219	-0.0333	0.0214
0.6523	0.4547	1.3301	-0.0297	0.0133
0.8085	0.4923	1.2158	-0.0179	-0.0004
1	0.5419	1.0929	0	0

It is evident that the plots of z_{im}^{E} *versus* mole fraction (x_1) of 2-EH are opposite in nature to those of the L_f^E plots. Table 5.8 shows that while the specific acoustic impedances (z_{im}) decrease, the intermolecular free lengths (L_f) increase as the mole fraction (x_1) of 2-EH in the mixtures increase. The magnitude of the intermolecular free lengths (L_f) has the order: (2-EH + DCE) > (2-EH + EDA) > (2-EH + MEA); this indicates that the molecular interactions between dissimilar molecules is also decreasing in the same order. The results, therefore, suggest the order of molecular interactions: (2-EH + MEA) > (2-EH + EDA) > (2-EH + DCE), which has already been discussed earlier.

5.3.8. ***Prediction of ultrasonic speed of sound***

The speeds of sound were predicted theoretically using the Collision factor theory (CFT), Nomoto relation (NOM), Impedance dependence relation (IDR), Ideal mixture relation (IMR) and Jungie (JUN). The details of these empirical models and method of calculation are described in chapter II. Theoretically calculated speeds of sound were correlated with the experimentally obtained ultrasonic speeds and the predictive capabilities of these models were judged on the basis of the percent standard deviations (σ%). The comparison of the σ% values has been depicted for each studied binaries in Figure 5.9. Figure 5.9 clearly reveals that the predictive capabilities of the different models used follow the order: CFT > IDR > IMR > NOM > JUN (for 2-EH + EDA mixture); NOM > CFT > JUN > IDR > IMR (for 2-EH + DCE mixture) and IDR > CFT > IMR > NOM > JUN (for 2-EH + MEA mixture), respectively.

5.3.9. ***Excess molar refractions***

Refractive indices can often be correlated with densities, surface tension and dielectric permittivity. That is why refractive index data along with other parameters derived from it provide valuable information regarding the molecular interactions in the liquid mixtures. For example, molar refraction is a volumetric property and thus excess molar refractions (R_m^E) can equally shed light on the molecular interactions in a multi-component liquid mixture like excess molar volumes. Hence the experimental refractive indices and densities at 298.15 K were utilized to evaluate the molar refraction and the excess molar refraction with the help of the following standard relations:[48]

$$R_m = \left[\frac{n_D^2 - 1}{n_D^2 + 2}\right] V_m \quad (31)$$

$$R_m^E = R_m - [x_1 R_{m,1} + x_2 R_{m,2}] \quad (32)$$

The experimental refractive indices, molar refractions and excess molar refractions for the three binaries under investigation at 298.15 K are presented in Table 5.9. The experimental refractive indices (n_D) were in good agreement with literature values[8,12,49,50] at 298.15 K. Table 5.9 manifests that R_m^E values are negative for the mixtures (2-EH + EDA) and (2-EH + MEA) over the entire composition range but such values vary slightly in a sigmoidal fashion for the mixture (2-EH + DCE). While the negative excess molar refractions suggest the solvent-solvent interactions, positive excess molar refractions suggest the presence of the dispersion forces between the unlike components in the mixtures.[51,52] Thus these results are also in good agreement with those obtained earlier from other excess or deviations properties.

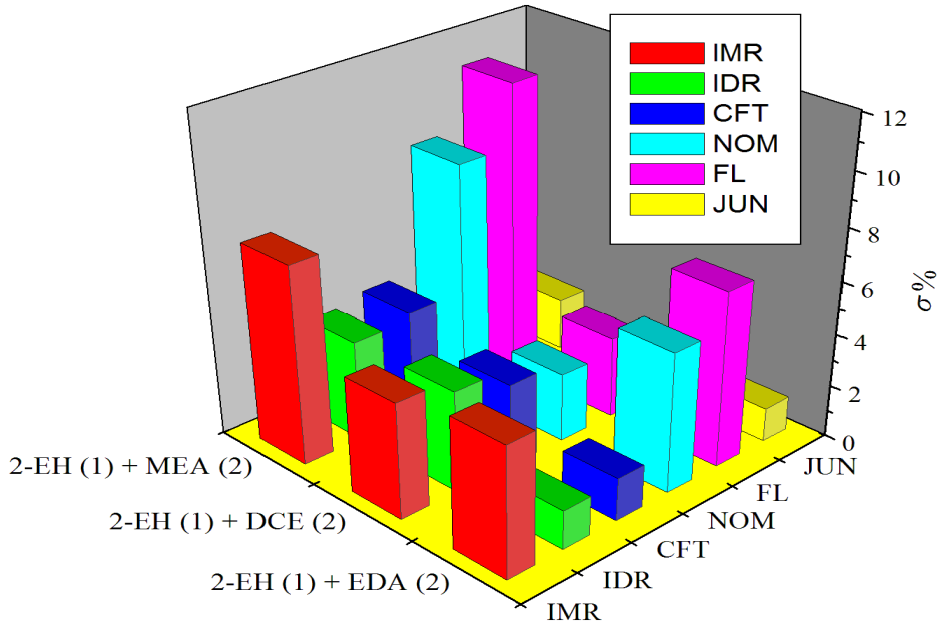

Fig. 5.9. Percent standard deviations ($\sigma\%$) for theoretical prediction of ultrasonic speeds by different empirical relations at T = 298.15 K for the binary mixtures studied.

The experimental refractive indices of the studied binaries were also predicted using several empirical or semi-empirical models like Lorentz-Lorenz (LL), Arago-Biot (AB), Gladstone-Dale (GD), Eykma (EYK), Newton (NEW), Heller (HEL), Eyring-

Table 5.9. Refractive indices (n_D), molar refractions (R_m) and excess molar refractions (R_m^E) for the binary mixtures at 298.15 K

x_1	n_D	$R_m \cdot 10^6$ ($m^3 \cdot mol^{-1}$)	$R_m^E \cdot 10^6$ ($m^3 \cdot mol^{-1}$)
2-EH (1) + EDA (2)			
0	1.4541	18.189	0
0.0488	1.4515	19.272	-0.006
0.1034	1.4488	20.478	-0.020
0.1651	1.4462	21.838	-0.037
0.2352	1.4438	23.391	-0.049
0.3157	1.4416	25.186	-0.051
0.4090	1.4392	27.259	-0.061
0.5185	1.4369	29.704	-0.059
0.6486	1.4345	32.620	-0.048
0.8059	1.4321	36.167	-0.013
1	1.4292	40.512	0
2-EH (1) + DCE (2)			
0	1.4419	21.006	0
0.0779	1.4428	22.531	0.006
0.1597	1.4406	24.124	0.004
0.2457	1.4386	25.793	-0.005
0.3363	1.4369	27.546	-0.019
0.4318	1.4353	29.400	-0.029
0.5327	1.4338	31.356	-0.041
0.6394	1.4326	33.441	-0.038
0.7525	1.4314	35.653	-0.030
0.8724	1.4304	38.008	-0.015
1	1.4292	40.512	0
2-EH (1) + MEA (2)			
0	1.4521	16.289	0
0.0495	1.4498	17.471	-0.017
0.1049	1.447	18.791	-0.041
0.1674	1.4447	20.281	-0.063
0.2382	1.4425	21.978	-0.081
0.3193	1.4402	23.923	-0.100
0.4020	1.4386	25.920	-0.106
0.5225	1.4366	28.845	-0.100
0.6523	1.4345	32.009	-0.080
0.8085	1.432	35.829	-0.044
1	1.4292	40.512	0

John (EJ) and Weiner (WEI) as detailed in chapter II. The predictive capabilities of these models were ascertained by estimating the percent standard deviations ($\sigma\%$). The percent standard deviations were 0.03, 0.01 and 0.06 for the mixtures (2-EH + EDA), (2-EH + DCE) and (2-EH + MEA), respectively for most of the models used and this fact suggests predicted refractive indices were in good agreement with the corresponding experimental values at 298.15 K.

5.3.10. ***IR spectroscopic study***

The results obtained so far are also well reflected in FT-IR spectra of the binary mixtures (Figures 5.10-5.12). The spectra were recorded in a demountable KBr cell for liquid samples with spacer of path length of 0.5 mm at ambient temperature with a Perkin-Elmer Spectrum FT-IR spectrometer (RX-1). 2-EH, being a branched eight carbon alcohol, is a flexible molecule and have a number of thermally accessible geometric conformers. All these conformers contribute to its infrared spectrum with smooth bands.[53] The FTIR spectrum of 2-EH exhibits the following characteristic bands: i) fundamental C-H stretching vibrations in the range 2900-2880 cm^{-1}, different C-C stretching vibrations at 1038 cm^{-1}, different H-C-H bending vibrations at around 1463 and 1379 cm^{-1} and a broad O-H band around 3340 cm^{-1}.[55] DCE has characteristic peaks around 1232 cm^{-1} for *trans* conformer and two peaks around 1313 and 1285 cm^{-1} for *gauche* conformer.[54] The broad O-H band of 2-EH gradually became less broad and its intensity also decreased as the mole fraction of DCE increased for the mixture (2-EH +DCE). On the contrary the fundamental C-H stretching vibrations of 2-EH in the range 2900-2880 cm^{-1} gradually became more distinct and sharp. Also the bands at 1232, 1285 and 1313 cm^{-1} of DCE shifted slightly in peak position and intensity as the mole fraction (x_1) of 2-EH increased for this mixture. All these changes in the spectrum of the mixture (2-EH + DCE) suggest weak interactions between the components. However, for the mixture (2-EH + EDA) the N-H and N-CH_2 stretching bands (at around 3296 and 2855 cm^{-1}, respectively) of EDA become less intense and broad as the mole fraction (x_1) of 2-EH in the mixture increased. Again the –NH bending vibration[55] of EDA that appeared at 1598 cm^{-1} slowly shifted to higher frequency (from 1598 to 1600 cm^{-1}) with increasing mole fraction of 2-EH. This indicates formation of inter-molecular hydrogen bonds

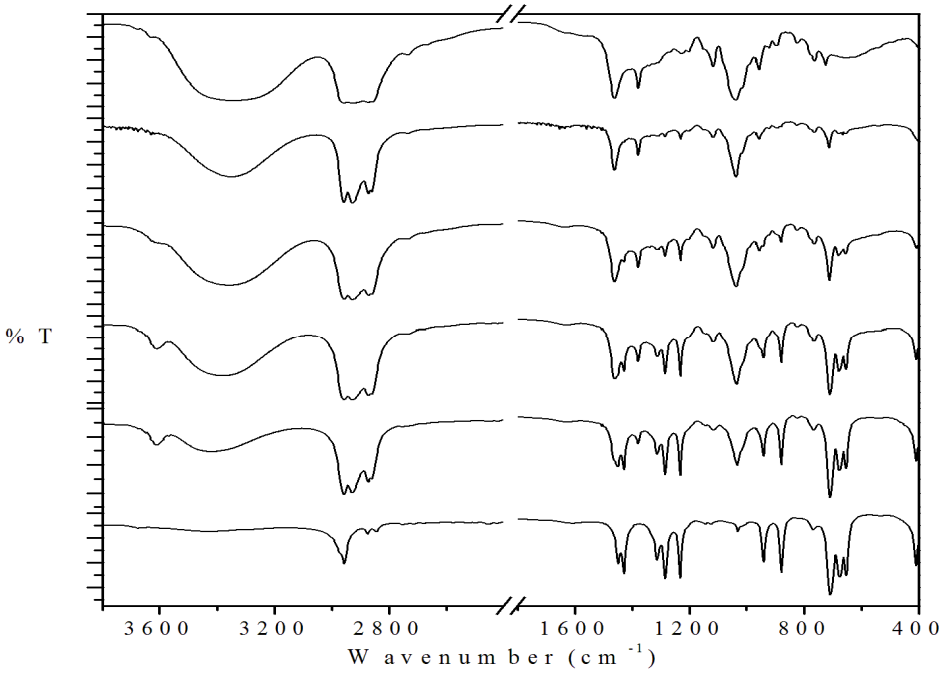

Fig. 5.10. FTIR spectra of the various binary mixtures of (2-EH + DCE): A, pure 2-EH (x_{DCE} = 0.00); B, (x_{DCE} = 0.20); C, (x_{DCE} = 0.40); D, (x_{DCE} = 0.60); E, (x_{DCE} = 0.80); F, Pure DCE (x_{DCE} = 1.00).

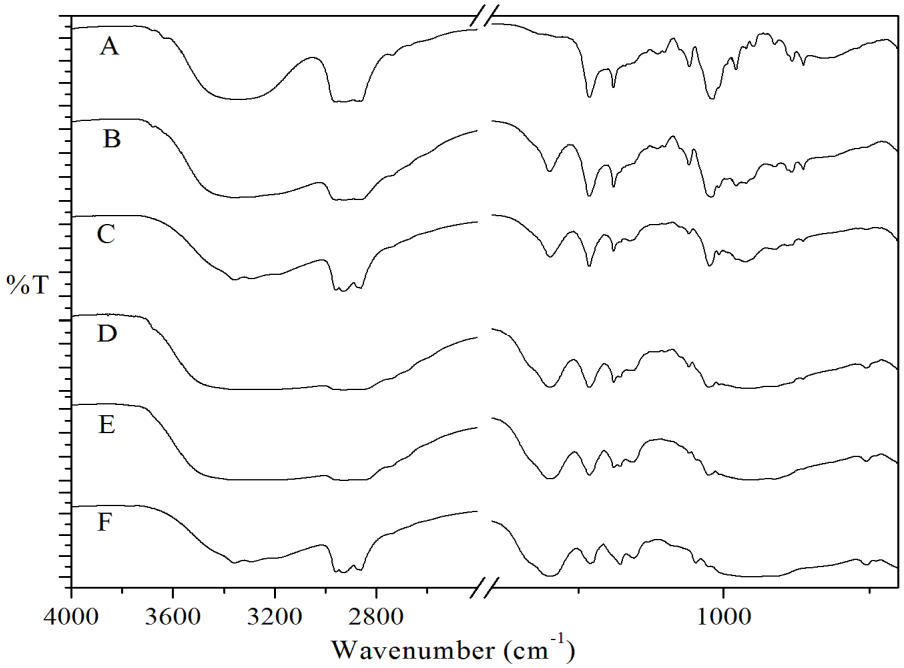

Fig. 5.11. FTIR spectra of the various binary mixtures of (2-EH + EDA): A, pure 2-EH (x_{EDA} = 0.00); B, x_{EDA} = 0.20; C, x_{EDA} = 0.40; D, x_{EDA} = 0.60; E, x_{EDA} = 0.80; F, Pure EDA (x_{EDA} = 1.00).

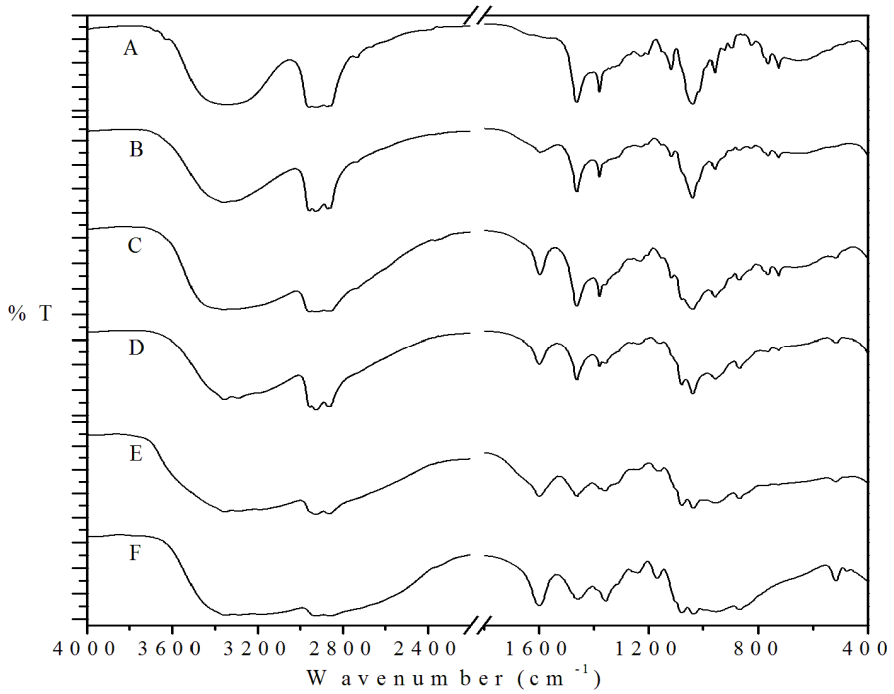

Fig. 5.12. FTIR spectra of the various binary mixtures of (2-EH + MEA): A, pure 2-EH (x_{MEA} = 0.00); B, x_{MEA} = 0.20; C, x_{MEA} = 0.40; D, x_{MEA} = 0.60; E, x_{MEA} = 0.80; F, Pure MEA (x_{MEA} = 1.00).

between dissimilar molecules in the mixture (2-EH + EDA). Similarly for the mixture (2-EH + MEA) the bands due to –OH and NH_2 groups (in the range 3335-2850 cm^{-1}) became much broader and their intensity decreased significantly as the mole fraction (x_1) of 2-EH decreased in the mixture. Also the fundamental C-H stretching vibrations of 2-EH gradually became less intense and broad, almost overlaps with the broad bands of –OH and $–NH_2$ groups. These spectral changes definitely suggest that the mixtures are characterized by intra-molecular and inter-molecular hydrogen bonds.

5.4. Conclusion

The densities, viscosities, ultrasonic speeds of sound and refractive indices for the binary mixtures of 2-EH with EDA, DCE and MEA at 298.15, 308.15 and 318.15 K over the entire composition range were determined. From the experimental data, the excess volumes (V_m^E), viscosity deviations ($\Delta\eta$), excess molar refractions (R_m^E) and different excess acoustic parameters like excess isentropic compressibility (κ_S^E), excess intermolecular free length (L_f^E) and excess acoustic impedance (z_{im}^E) were

obtained. The reported excess or deviation properties show both positive and negative deviations from ideal ones and their variations with mole fraction (x_1) of 2-EH were discussed in terms of molecular interactions like dipole-dipole interactions, hydrogen bond formation and interstitial accommodation, *etc*. This study revealed that the molecular interaction is highest in the mixture (2-EH + MEA) and least in the mixture (2-EH + DCE) and thus the order of molecular interactions follows the order: (2-EH + MEA) > (2-EH + EDA) > (2-EH + DCE). These excess molar volumes were correlated by using PFP, PREOS models and viscosities were correlated using PREOS and Bloomfield-Dewan models. FTIR spectra of the mixtures showed characteristic band shifts in position and intensity reflecting the nature of molecular interaction in the studied mixtures.

References

[1] A. Ali, H. Soghra, Ind. J. phys., 76 (2002) 23.

[2] A. Ali, A.K. Nain, N. Kumar, M. Ibrahim, J. Pure Appl. Ultrason., 24 (2002) 27.

[3] R. Mehra, R. Israni, Ind. J. Pure Appl. Phys., 38 (2000) 81.

[4] S.I. Oswal, N.B. Patel, J. Chem. Eng. Data 40 (1995) 845.

[5] B. Gracia, R. Alcalde, J. M. Leal, J. Chem. Soc., Faraday Trans., 93 (1997) 1115.

[6] G.A. Krestov, *Thermodynamics of Solvation*, Ellis Horwood, England, (1991) pp.151.

[7] M.I. Aralaguppi, C.V. Jadar, T.M. Aminabhavi, J. Chem. Eng. Data 44 (1999) 446.

[8] A.M. Awwada, R.A. Pethric, J. Chem. Soc. Faraday Trans. I, 78 (1982) 3203.

[9] E. Zorebski, M. Dzida, E. Wysocka, J. Chem. Eng. Data 56 (2011) 2680.

[10] S.C. Bhatia, J. Sangwan, R. Rani, V. Kiran, Int. J. Thermophys., 34 (2013) 2076.

[11] C. Li, J. Zhang, T. Zhang, X. Wei, E. Zhang, N. Yang, N. Zhao, M. Su, H. Zhou, J. Chem. Eng. Data 55 (2010) 4104.

[12] J.K. Gladden, J. Chem. Eng. Data 17 (1972) 468.

[13] M.A. Saleh, M.S. Ahmed, M.S. Islam, Phys. Chem. Liq., 40 (2002) 477.

[14] R. Pradhan, A. Kamath, D. Brahman, B. Sinha, Fluid Phase Equilib., 404 (2015) 131.

[15] S. Ranjbar, K. Fakhri, B. Jahan, J. Ghasemi, J. Chem. Eng. Data 54 (2009) 3284.

[16] R.K. Biswas, R.A. Banu, M.N. Islam, Hydrometallurgy, 69 (2003) 157.

[17] S.E. Burke, B. Hawryla, R. Palepu, Thermochim. Acta., 345 (2002) 101.

[18] U.R. Kapadi, D.G. Hundiwale, N.B. Patil, M.K. Lande, Fluid Phase Equilib., 201 (2002) 335.

[19] Y. Mahan, C.N. Liew, A.E. Mather, J. Solution Chem., 31 (2002) 743.

[20] W.M. Haynes, D.R. Lide, T.J. Bruno, *CRC Handbook of Chemistry & Physics*, 93rd edn., Taylor & Fransis¸ Boca Roton, London, 2012-2013.

[21] S.C. Bhatia, R. Bhatia, G.P. Dubey, J. Mol. Liq., 144 (2009) 163.

[22] G.M. Smith, H.C. Van Ness, *Introduction to Chemical Engineering Thermodynamics*, McGraw Hill, New York, 1987.

[23] H.A. Zarei, J. Mol. Liq., 130 (2007) 74.

[24] O. Redlich, A.T. Kister, Indus. Eng. Chem., 40 (1948) 345.

[25] D.W. Marquardt, J. Soc. Ind. Appl. Math., 11, (1963) 431.

[26] D. Patterson, G. Delmas, J. Polym. Sci., 30 (1970) 1.

[27] D. Patterson, Pure. Appl. Chem., 47 (1976) 305.

[28] P.J. Flory, R.A. Orwell, A. Vriji, J. Am. Chem. Soc., 86 (1964) 3507.

[29] P.J. Flory, R.A. Orwell, A. Vriji, J. Am. Chem. Soc., 86 (1964) 3515.

[30] P.J. Flory, J. Am. Chem. Soc., 87 (1965) 1833.

[31] A. Abe, P.J. Flory, J. Am. Chem. Soc., 87 (1965) 1838.

[32] D.Y. Peng, D.B. Robinson, Ind. Eng. Chem. Fundum., 15 (1976) 59.

[33] S.I Sandler, *Chemical, Biochemical, and Engineering Thermodynamics*, 4th edn, John Wile & Sons (Asia), New Delhi, 2006, pp. 242, 258.

[34] M.A. Saleh, S. Akhtar, M.S. Ahmed, Phys. Chem. Liq., 44 (2006) 551.

[35] S. Glasstone, K.J. Laidler, H. Eyring, *The theory of Rate Preocess*. McGraw-Hill Book Comnpany, Inc., New York, 1941.

[36] R.J. Fort, W.R. Moore, Trans. Faraday Soc., 62 (1966) 1112.

[37] H. Vogel, A. Weiss, Phys. Chem. Chem. Phys., 86 (1982) 193.

[38] F. Corradini, L. Marcheselli, A. Marchetti, M. Tagliazucchi, L. Tassi, G. Tosi, Bull. Chem. Soc. Jpn., 65 (1992) 503.

[39] T.M. Reid, T.E. Taylor, J. Phys. Chem., 63 (1959) 58.

[40] A.K. Mehrotra, W.D. Monnery, W. Svrcek, Fluid Phase Equilib., 117 (1996) 344.

[41] R.D. McCarty, Fluid Phase Equilib., 256 (2007) 42.

[42] V.A. Bloomfield, R.K. Dewan, J. Phys. Chem., 75 (1971) 3113.

[43] J.S. Rowlinson, F.L. Swinton, *Liquid and Liquid Mixtures*, Butterworths, London, 3rd edn., 1982, pp. 16,17.

[44] G.P. Dubey, K. Kumar, J. Chem. Eng. Data 56 (2011) 2995.

[45] S.C. Bhatia, R. Bhatia ·G.P. Dubey, Int. J. Thermophys., 31(2010) 2119.

[46] G.C. Benson, O.K. Kiyohara, J. Chem. Thermodyn., 11 (1979) 1061.

[47] W.E. Acree, J. Chem. Eng. Data 28 (1983) 215.

[48] A. Ali, A.K. Nain, D. Chand, R. Ahmad, J. Chin. Chem. Soc., 53 (2006) 531.

[49] K.M. Kadish, J.E. Anderson, Pure. Appl. Chem., 59 (1987) 703.

[50] M. Yasmin, M. Gupta, J. Solution Chem., 40 (2011) 1458.

[51] A. Pineiro, P. Brocos, A. Amigo, M. Pintos, R, J. Chem. Thermodyn., 31 (1999) 931.

[52] D.S. Wankhede, Int. J. Chem. Res., 2 (2011) 23.

[53] T.N. Clasp, S.W. Reeve, H. Koizumi, J. Theo. Comp. Chem., 16 (2017) 1750023.

[54] R.K. Sreeruttun, R. Ramasami, Phys. Chem. Liq., 44 (2006) 315.

[55] Q. Li, F. Sha, G. Zhao, M. Yang, L. Zhao, Q. Zhang, J. Zhang, . Chem. Eng. Data 61 (2016) 1718.